Technical Paper

Finite element analysis of overlaid UHPFRC-strengthened steel bridge deck under moving wheel load

Chi Hieu MA*, Pengru DENG**, Hiroshi MITAMURA***, Takashi MATSUMOTO****

*Doctoral student, Graduate School of Engineering, Hokkaido University
(Kita 13, Nishi 8, Kita-ku, Sapporo 060-8628, Japan)
**Assistant Professor, Faculty of Engineering, Hokkaido University
(Kita 13, Nishi 8, Kita-ku, Sapporo 060-8628, Japan)
***J-THIFCOM Construction Association
(Kouraibashi 4-5-13, Chuo-ku, Osaka 541-0043, Japan)
****Professor, Faculty of Engineering, Hokkaido University
(Kita 13, Nishi 8, Kita-ku, Sapporo 060-8628, Japan)

This study presents a numerical method developed in the finite element model to analyze the fatigue behaviors of the orthotropic steel bridge deck strengthened with the overlaid UHPFRC under moving wheel load. In this method, the bridging stress degradation concept is applied as a primary mechanism in the fatigue crack growth generated in UHPFRC. From the analysis, the behavior evolutions, e.g. strain, displacement, and crack propagation in UHPFRC, are investigated. The analytical results show an acceptable agreement with the experimental data, and this numerical method can be used for the fatigue analysis of the UHPFRC-steel composite deck subjected to a repetitive traffic load.

Keywords: UHPFRC-steel composite deck, bridging stress degradation, fatigue, inter--face debonding, running wheel load

1. INTRODUCTION

In recent years, fatigue deterioration has been reported in the Orthotropic Steel Decks (OSD), which is a popular structure used in many large span bridges. Due to the small thickness of deck plates from early state design, fatigue cracks can initiate and propagate at the high-stress locations, i.e. welded connection joints, of the OSD subjected to heavy traffic loading. Therefore, it is essential to develop the effective rehabilitation methods to reduce the stress level in steel deck plate for prolonging the fatigue lives of the existing OSD structures. One promising method for addressing this need is to overlay a strengthening layer of Ultra High-Performance Fiber Reinforced Concrete (UHPFRC) on the top surface of steel deck plate. The UHPFRC with superior properties, i.e. high strength, a tensile strain-hardening behavior and low permeability that resists against the chloride ion and water ingress, exhibits the advantage in reducing internal stress and improving the overall stiffness of the OSD[1]. To date, the investigations of the UHPFRC-steel decks are primarily based on the experimental approach. This leads to the necessity to propose a reliably analytical procedure that can be conveniently applied to analyze the fatigue performance of the real OSD structures strengthened with UHPFRC.

In this study, a finite element analysis based on bridging stress degradation is performed to simulate the fatigue behaviors of the OSD with the UHPFRC reinforced overlay under moving wheel loads. Strain evolutions at the critical positions are considered and compared with the experimental results. It is found that the fatigue numerical results of UHPFRC-steel composite deck under moving load shows an acceptable agreement with those from experiment.

2. METHODS

2.1 Analytical model

In this study, a three-dimensional nonlinear finite element analysis based on bridging stress degradation is performed by using a FEM software, i.e. MSC/MARC, to simulate the OSD with UHPFRC reinforced overlay under moving wheel load. Cracking behaviors of UHPFRC, i.e. crack formation and propagation, are represented by 3D eight-node smeared crack elements relied on the multiple fixed crack concept[2]. The initiation of cracks is based on the direction and magnitude of the maximum principal stress generated in UHPFRC overlay. When the tensile stress reaches the cracking strength of UHPFRC, the first crack forms in the matrix perpendicularly to the direction of the maximum principal stress. Similarly, the second and third cracks can initiate perpendicular to the first crack when the second and third components of tensile stress exceed the cracking stress of UHPFRC. The total strain in cracked material is decomposed into the cracked component and non-cracked component in this approach. Finally, the global stress-strain relationship consisting of the elastic and cracked stiffness matrices of UHPFRC can be obtained following the procedure proposed by Rots and Blaauwendraad[2]. Due to no experimental report about fatigue failure of steel members, the fatigue of steel components is not considered in the analysis.

2.2 Material model

(1) Steel

The constitutive law of steel is represented by a bilinear isotropic hardening material as showed in Fig. 1. The main properties of steel material, i.e. yield strength and maximum tensile strength, are listed in Table 1. The yield criterion in the model is following to von Mises' law. The Poisson's ratio and Young's modulus are 0.3 and 200 GPa, respectively, in this study.

(2) UHPFRC

The constitutive relationship of UHPFRC is defined in a material user subroutine by using programming language FORTRAN. Following the Recommendations for Design and Construction of High-Performance Fiber Reinforced Cement Composites with Multiple Fine Cracks (HPFRCC) [3], the stress-strain law of UHPFRC in both compression and tension are chosen as shown in Fig. 2. As mentioned in section 2.1, in the fixed smeared crack approach, the stress-strain relationship of the cracked body is defined by non-cracked and cracked components. For the non-cracked component of UHPFRC, the linear elastic isotropic relationship is defined as represented in Fig. 2(a). The Poisson's ratio and Young's modulus of 0.22 and 31.3 GPa are used for the elastic state of UHPFRC in the analysis. In Fig. 2(b), the constitutive law for the cracked component is defined by a bilinear relationship in tension, i.e. strain hardening and strain softening. Stress-strain law for cracked component in compression is presented by a parabolic relationship. The material properties of UHPFRC are listed in Table 2 according to the experimental design. In fixed crack model, the crack orientation is maintained constant during entire computational process. The principal stress directions changing with wheel load moving are decomposed into tensile and shear components in accordance with initial crack orientation. Referring to the observation of cracks under tensile unloading in fiber composite specimens[4], the totally crack closure can not be attained at the zero-strain level due to the resistance of the pulled-out fibers that are pushed back into matrix or buckled between crack surfaces. Following this observation, the unloading behavior for the stress-strain cracked component is then applied as illustrated in Fig. 2(b).

Considering shear components before cracking, the elastic shear modulus is used for UHPFRC. After crack initiates, shear retention factor, γ, is introduced in the analysis as follow

$$\gamma = \frac{1}{1 + \beta \varepsilon_{t\max}} \tag{1}$$

where ε_{tmax} is maximum tensile strain, coefficient β = 4447 is chosen in this study referring to Fairbairn et al.[5].

The bridging stress degradation relation is considered as a primary degradation mechanism in the propagation of fatigue crack in normal concrete and fiber reinforced concrete. Under fatigue action, the deterioration of fiber components, i.e. fiber fatigue rupture and matrix/fiber pullout, leads to the gradual degradation of bridging stress between crack surfaces.

Table 1. Material properties of steel

Member	Type	Yield strength, f_y (MPa)	Tensile strength, f_u (MPa)
Steel deck plate	SM490YA	365	490
Longitudinal bulb rib	SM490YA	365	490
Cross beam	SM400YA	245	400

Table 2. Material properties of UHPFRC

Point	Material properties		Values (unit)
1	Tensile initial cracking	σ_{cr}	6 (MPa)
		ε_{cr}	0.00019
2	Tensile strength	σ_{t0}	9 (MPa)
		ε_{t0}	0.00175
3	Ultimate tensile strain	ε_{tu}	0.01200
4	Compressive strength	σ_{cu}	133 (MPa)
		ε_{cu}	0.0085

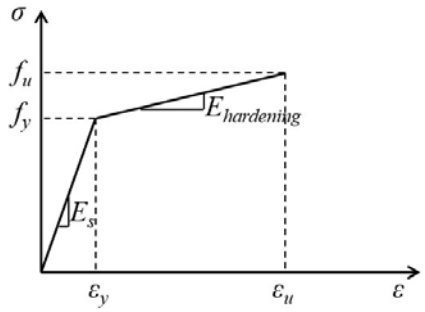

Fig. 1 Stress-strain relation of steel

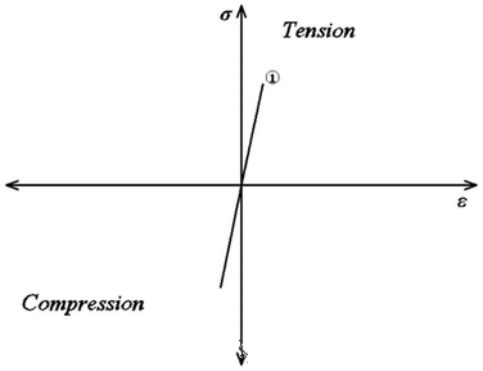

(a) Non-cracked component

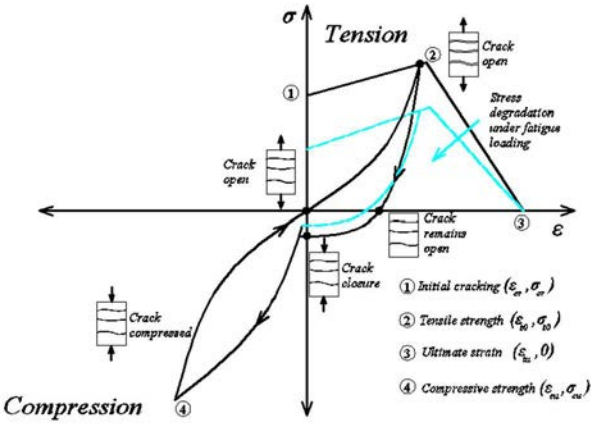

(b) Cracked component

Fig. 2 Constitutive law of UHPFRC

According to the study of Li and Matsumoto[6], the bridging stress degradation can be simply assumed by a function of two parameters, i.e. maximum tensile strain ε_{tmax} and number of cycle N. For the material model of UHPFRC under tensile fatigue loading, the degradation law can be expressed by

$$\frac{\sigma_N}{\sigma_1} = f(\varepsilon_{t\max}, N) \le 1$$
$$\frac{\sigma_N}{\sigma_1} = 1 - (a_0 + a_1 \varepsilon_{t\max}) \log(N) \quad (1)$$

where σ_N/σ_1 is bridging stress ratio between the N^{th} and the first cycles, a_0 and a_1 are the coefficients depending on the material. Since there is insufficient data considering the bridging stress degradation of UHPFRC, the degradation rate will be determined by the trials of the coefficients a_0 and a_1 in the analysis until the FEM results fit with those from experiment. In this study, the coefficients a_0 and a_1 are chosen as 0.035 and 5, respectively. These coefficients for UHPFRC give a reasonable degradation rate which is usually equal to 0.5 – 0.6 for concrete material at the 1,000,000th loading cycle.

2.3 Details of composite deck

(1) Geometric description

As illustrated in Fig. 3(a), the strengthened OSD is composed of the UHPFRC overlay, steel deck plate, main girders, cross beams and longitudinal open bulb ribs. The dimensions of the deck plate are 3300 and 2720 mm in longitudinal and transverse directions, respectively. The steel deck with a thickness of 12 mm is overlaid by a 25 mm layer of UHPFRC. The main girder has an average depth of 690 mm and a thickness of 14 mm. The steel deck plate is stiffened by 7 longitudinal bulb ribs with a size of 230×11×30 mm and 3 cross beams with 9 mm web thickness. The bond layer connecting steel plate and UHPFRC is not considered in this analysis, and the steel/UHPFRC interface is assumed to be perfectly bonded with no existence of sliding by applying the contact GLUE option in Marc program. The bottom layer of UHPFRC and the top surface of the steel plate are defined as the deformable bodies under mutually glue interaction specified in a CONTACT TABLE option.

(2) Boundary conditions

The boundary conditions of the composite deck are shown in Fig. 3(d). Four outer edges of the main girders are simply supported on a 3000-mm span. The pattern of the wheel loading lane is simulated as 2 paths along the longitudinal direction with the range of ± 875 mm from the midspan. The distance between two loading paths representing the gap between two rubber tires is set as 110 mm in the middle of the transverse side. A total of seven distributed loads with a size of 2×220×250 mm, which is assumed as a rubber tire contact area, are assigned along the loading lane with the level of 100 kN referring to the experimental design.

2.4 Procedure of fatigue analysis under moving wheel load

For one cycle of fatigue analysis, the wheel load is firstly applied at the center position. After reaching the peak from zero, these elements are unloaded at the same time with the starting of the loading process from the adjacent location with an equal augmented rate. Applying this procedure along the loading lane, one cycle of fatigue analysis including a total of 13 load cases is finally completed at the center position again

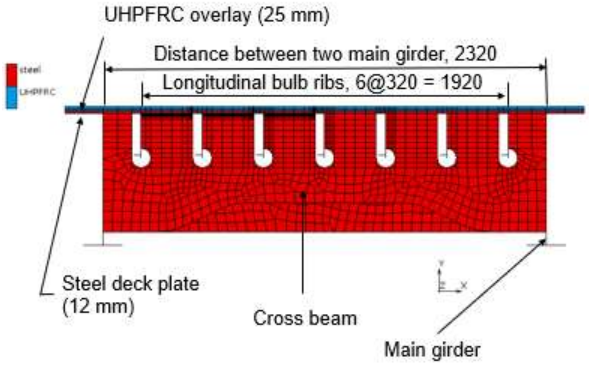

(a) Front view of bridge deck

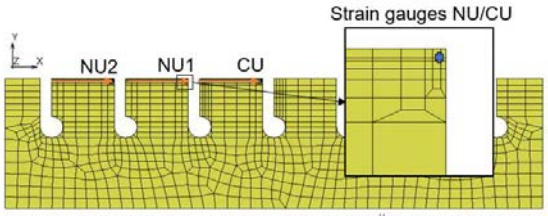

(b) Middle cross beam

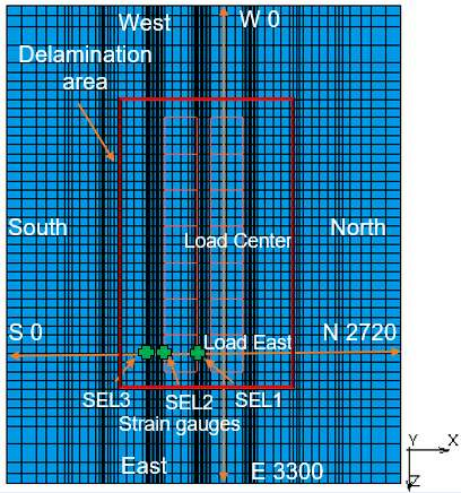

(c) Top view of bridge deck

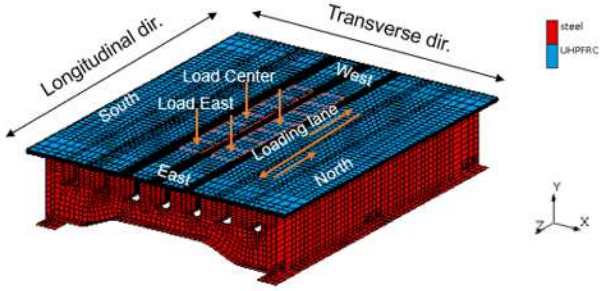

(d) Wheel loading lane

Fig. 3 Geometry of UHPFRC-steel composite deck

(Fig. 3(d)). After finishing one cycle of moving load, the data of the maximum tensile strain and cracking state at each node of 3D smeared crack elements in UHPFRC are recorded. Subsequently, for the following cycle of fatigue analysis, the history maximum tensile strains are read and applied in the bridging stress degradation equation coded in the user subroutine. The tensile strength of UHPFRC is then modified that causes the decrease in stiffness and appearance of new cracks in the strengthening overlay. The procedure is continued until the number of cycles reaches 1,100,000 when the experiment in dry condition of composite deck under moving wheel load completes.

3. RESULTS AND DISCUSSIONS

In the analysis, the strain behavior evolutions in the OSD strengthened with the UHPFRC overlay under moving wheel load are examined from some citical locations that are obtained from experiment and the static analsysis as listed in the Table 3.

3.1 Strain evolution under the bottom of steel deck plate

In Fig. 4, relationships between the strain evolutions in transverse direction and the number of cycles obtained from points SEL1 are presented comparatively with those from the experiment. Positions of strain gauge SEL1 under the bottom of steel deck plate are displayed in Fig. 3(c). Due to the progressive cracks caused by bridging stress degradation in UHPFRC, the stiffness of composite deck decreases with the increase of loading cycles. This leads to the continuous increase in strain levels under the steel deck plate. From the first cycle to 700,000th cycle, the strain results collected from point SEL1 slightly change from 104.45μ to 108.59μ. Until the 700,000th loading cycles, the analytical strain results relatively fit with the experimental data. From the 700,000th to 1,100,000th loading cycles, the sharp increases in transverse strain levels obtained from three gauge-points SEL1, SEL2 and SEL3 are observed in the experiment. The reason may due to the delamination of the UHPFRC/steel interface. To clarify this assumption, the FEM model at the interface between two materials has been modified from perfect adhesive connection to total slip regime under the loading lane regions. GLUE DEACTIVATION option is applied at the material interface, that automatically modifies the contact interaction from GLUE

Table 3. Critical locations in composite deck

Member	Critical position	Load position	Strain direction
Steel deck plate	Middle point of path SN (Fig. 3(c))	Load East	X direction
Middle crossbeam	Strain gauge NU1	Load Center	Y direction
UHPFRC layer	Middle point of path SN	Load East	X direction

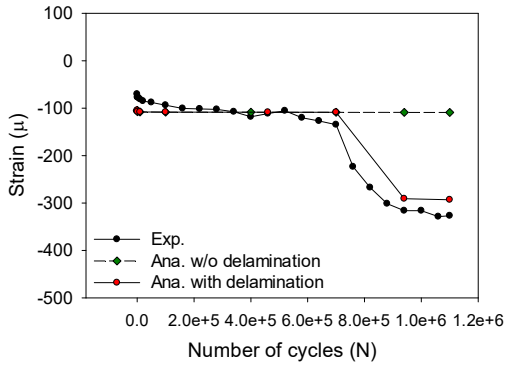

Fig. 4 Strain evolutions in X direction at strain gauge SEL1

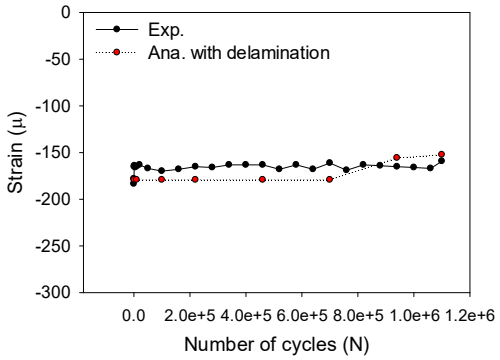

Fig. 5 Strain evolution in Y direction at strain gauge NU1

to TOUCHING. Total slip regime is then assumed after glue breaking in TOUCHING contact by specifying the zero value of friction coefficient. In the real case, the friction coefficient between UHPFRC and steel materials is of region between 0 and 1. Hence, the friction coefficient between two materials after delamination is also a topic for further study. In this study, the delamination area of 1210×2250 mm (transverse × longitudinal) chosen as shown in Fig. 3(c). When the debonding area is under compressive loading, the UHPFRC overlay and the steeldeck plate are in contact without frictional action, and the stresses can still be transferred between the two materials with the prevention of material penetration in the analysis. On the contrary, as the delamination area is under tensile mode, the separation between UHPFRC and steel occurs. Consequently, the stresses in UHPFRC under moving load are transferred into adjacent UHPFRC elements instead of the steel deck plate below. This leads to the strain re-distribution causing the increase of strain levels under steel deck as well as UHPFRC. It is found that the analytical strain level in transverse direction significantly increases at the 940,000th loading cycle after the interface debonding (from -108.59μ to -291.02 μ at point SEL1). In Fig. 4, it can be observed that strain results from the model with delamination exhibit acceptable agreement with the experimental data.

3.2 Strain evolution on the middle cross beam

The strains in Y direction versus the number of cycles are obtained at points NU1 (Fig. 3(b)) under load Center, and compared with those from the experiment, as showed in Fig. 5. With the increase of the analysis cycles, the strain levels at gauge point NU1 gradually increase from -178.13μ to -179.21μ at 700,000th loading cycle, which is resulted by the progressive deterioration in UHPFRC. After the interface delamination, the analytical strain notably changes to -155.67μ. The strain result from analysis is more sensitive to the strain re-distribution of deck plate than the experimental one. The reason may be due to the lack of welding between steel plate and middle cross beam in the finite element analysis. This causes the reduction in stiffness at the vicinity of connection parts between the steel members.

3.3 Strain evolution on top surface of UHPFRC

The strains in X direction obtained on top surface of the UHPFRC layer from the middle point of path SN are plotted versus the number of cycles in Fig. 6. Owing to the separation of strain gauges and UHPFRC surface after 20,000th load cycle, only analytical results are discussed in this section. After the comparative large slope of strain increase in the initial stage, the slope gradually increases to the 700,000th load cycle. At the cycle 940,000th, the remarkable increase in strain level of UHPFRC is obtained due to the combination of the two kinds of degradations: fatigue bridging stress degradation and interface debonding. From the cycles 940,000th to 1,100,000th, the strain behavior is influenced by only fatigue degradation of bridging stress in UHPFRC since the delamination area keeps unchanged. However, the UHPFRC strain unexpected drops at the end of analysis. This may happen because the slip occurs between two materials as resulted by the frictionless definition in the FEM after debonding.

As observed in the early state of fatigue analysis, there is a relatively large difference between the numerical numerical and experimental results. This is caused by the limitation of

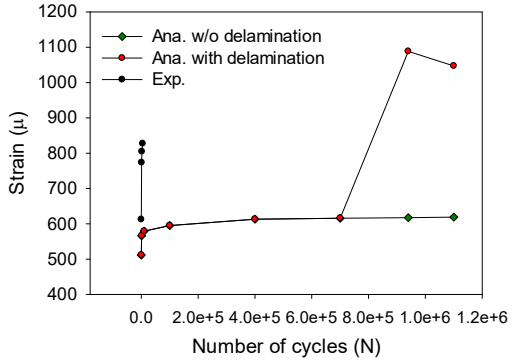

Fig. 6 Strain evolution in X direction at the middle of path SN

FEM when the local deformation in the region above the middle stiffener can not be sufficiently captured by the fine mesh in the analytical model. To deal with this issue, a weak-performance UHPFRC material may be used in further study for a better reproduction of the local behavior in the regions above the longitudinal stiffeners.

3.4. Maximum principal strain on the UHPFRC surface

In Fig. 7, the tensile strain distribution and crack regions under load East obtained on the top surface of UHPFRC overlay are displayed at the first cycle and the finished cycle with and without delamination. The cracked areas in UHPFRC are represented by grey color. From the model without material debonding, the in-plane crack regions slightly expand at the end of analysis. Considering the model with delamination, it is noticed that not only tensile strain magnitudes but also the speed of fatigue crack growth exhibit higher values than those from the model without interface failure. Therefore, a larger crack area is obtained from top surface of UHPFRC when the interface debonding is taken into consideration in the analysis.

4. CONCLUSIONS

In this study, the fatigue analysis of OSD strengthened overlaid UHPFRC under repetitive loading is proposed based on the bridging stress degradation concept. The non-linear FEM model using three-dimensional smeared crack elements is performed to predict fatigue behavior of the composite deck subjected to moving wheel load. Referring to the experimental fatigue performance of UHPFRC-steel bridge deck, the interface delamination may occur from the 700,000th loading cycle. Therefore, the analytical fatigue behavior of bridge deck is governed by two degradation stages:

- First stage (from beginning to 700,000th cycle): continuous crack in UHPFRC due to fatigue bridging stress degradation.
- Second stage (from the cycles 700,000th to 1,100,000th): progressive crack in UHPFRC caused by fatigue bridging stress degradation and stress re-distribution after interface delamination.

It is found that the analytical strain results from the bridge deck model considering interface degradation show acceptable agreement with those from the experiment.

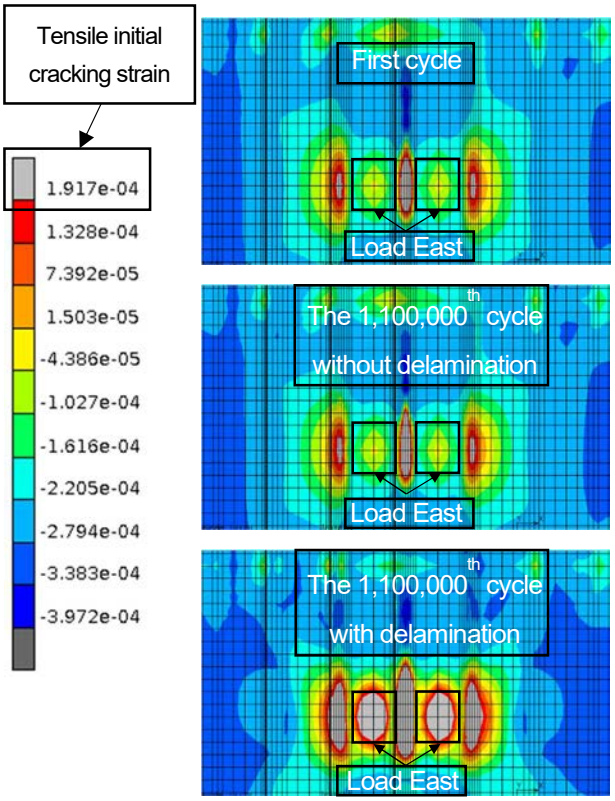

Fig. 7 Maximum principal tensile strain distribution and crack formation under load East

ACKNOWLEDGEMENT

This work has been supported by the Kajima Foundation's International Joint Research Grant. Their support is gratefully acknowledged by the authors.

REFERENCES

1) Manabe, H., Huang, C. W., Kosaka, Y., Mitamura, H., Matsumoto, T. and Imai, T.: Verification of repair effect of bridge deck using UHPFRC (J-THIFCOM), 12th Japanese German Bridge Symposium, Universität München, 2018.
2) Rots, J. G. and Blaauwendraard, J.: Crack models for concrete: discrete or smeared? Fixed, multi-directional or rotating?, HERON, Vol.34, No.1, pp. 1-59, 1989.
3) Japan Society of Civil Engineers (JSCE): Recommendations for Design and Construction of High Performance Fiber Reinforced Cement Composites with Multiple Fine Cracks (HPFRCC), JSCE, 2008.
4) Matsumoto, T., Wangsiripaisl, Hayashikawa, T. and He, X.: Uniaxial tension-compression fatigue behaviour and fiber bridging degradation of strain hardening fiber reinforced cementitious composites, International Journal of Fatigue, Vol.32, No.11, pp. 1812-1882, 2010.
5) Fairbairn, E. M. R., Toledo Filho, R. D., Battista, R. C., Brandao, J. H., Rosa, J. I. and Formagini, S.: Experimental and numerical analysis of UHPFRC plates and shells. Symposium of Measuring, Monitoring and Modeling Concrete Properties, pp. 49-58, Springer, Dordrecht, 2006.
6) Li, V. C. and Matsumoto, T.: Fatigue crack growth analysis of fiber reinforced concrete with effect of interfacial bond degradation, Cement and Concrete Composites, Vol.20, No.5, pp. 339-351, 1998.

(Received July 17, 2020)